

Tunable temperature induced magnetization jump in a GdVO₃ single crystal

L D Tung*

Department of Physics, University of Warwick,
Coventry CV4 7AL, United Kingdom.

(dated: 20 Dec. 05, accepted to be published in Physical Review B)

Abstract: We report a novel feature of the temperature induced magnetization jump observed along the a -axis of the GdVO₃ single crystal at temperature $T_M \approx 8$ K. Below T_M , the compound shows no coercivity and remanent magnetization indicating a homogenous antiferromagnetic structure. However, we will demonstrate that the magnetic state below T_M is indeed history dependent and it shows up in different jumps in the magnetization only when warming the sample through T_M . Such a magnetic memory effect is highly unusual and suggesting different domain arrangements in the supposedly homogenous antiferromagnetic phase of the compound.

PACS numbers: 75.50.Ee; 75.30.Kz; 75.60.Lr

* Email address Tung.Le@warwick.ac.uk

I. INTRODUCTION

The Mott insulating transition metal oxides are among systems with the richest physical properties. In the past decade or so, despite of increasingly worldwide efforts in the studies, understanding many anomalous properties of the Mott insulators is still at infancy. The RVO_3 compounds ($R =$ rare earth or Y) are Mott insulators which have some special characteristics. The magnetism of the compounds is driven mainly by the V^{3+} ions which have d^2 configuration with two electrons coupled ferromagnetically according to the Hund's rule. The two electrons can occupy two states of the degenerate triplet t_{2g} orbitals, and thus orbital quantum fluctuation (OQF) is expected. When cooling to temperature below T_{OO} (ranging from 141 K to ~ 200 K for different rare earths [1]), the RVO_3 compounds experience the orbital ordering (OO) transition which involves marked redistribution of the valence electron density. OO is usually driven by the Jahn-Teller (JT) lattice distortion which will lift the orbital degeneracy and suppress OQF. Recently, the central discussions on the RVO_3 compounds have been focused on OQF versus JT physics [2-5].

The RVO_3 compounds have been reported with numerous anomalous magnetic properties including temperature induced magnetization reversal [6-11], low field sensitive character [11,12], staircaselike hysteresis loops [12] etc. In the present paper, we will report a novel feature related to the magnetic memory effect observed along the a -axis of the $GdVO_3$ single crystal which have not been detected previously by earlier studies for polycrystalline [13-15] and single crystal sample [1].

II. EXPERIMENT

$GdVO_3$ single crystal was grown by means of the floating zone technique using a high temperature Xenon arc-furnace. Detail procedure of the crystal growth is similar to compounds with other rare earths which have been previously described [11,12].

Measurements of the *zero*-field-cool (*ZFC*) [Ref.16], field-cooled (*FC*) magnetization and the magnetic isotherms of the sample were carried out in a commercial SQUID magnetometer. In the *FC* measurements, the sample is cooled from paramagnetic region to 1.8 K in an applied field. In here, the data can be taken either on cooling (*FCC*) or on warming (*FCW*). For the *ZFC* measurements, the sample is cooled in *zero* field to 1.8 K before the magnetic field is applied. The data are then taken on warming. Heat capacity measurements of the sample were carried out in a Physical Property Measurement System (PPMS) using a heat capacity option.

III. RESULTS

In Fig. 1, we present the heat capacity C and C/T as a function of temperature for the compound. The OO transition occurs at $T_{OO} = 199$ K and then is followed by an antiferromagnetic (AF) spin ordering (SO) transition at $T_{SO} = 118$ K. In the ordering region below T_{SO} , we observed another transition at temperature T_M of about 8 K. Our heat capacity data are similar with those previously reported on single crystal sample by Miyasaka et al. [1].

The results of *FCC*, *FCW* magnetization of the GdVO_3 single crystal along the main axes are presented in Fig. 2. In here the *a*- *b*- and *c*-axes are defined according to the *Pbnm* orthorhombic lattice with the lattice parameters $a = 5.342 \text{ \AA}$, $b = 5.604 \text{ \AA}$, $c = 7.637 \text{ \AA}$ [17]. We would like to note that, for GdVO_3 , the data of the neutron diffractions measurements are not available due to the neutron absorbent nature of Gd. However, for other compounds with $R = \text{La-Dy}$, it is known from powder neutron diffraction results [18] that the magnetic structure is of C-type, i.e. the spins order antiferromagnetically in the *ab*-plane and ferromagnetically along the *c*-axis. Since Gd is in between La and Dy, it is therefore reasonable to assume also the C-type magnetic structure for the compound.

From Fig. 2, it can be seen that the two transitions at T_{SO} and T_M observed from the previous heat capacity data are again shown up in the magnetization data. At the OO temperature, we cannot detect any anomaly in the inversed susceptibility (Fig. 3). The Curie-Weiss behavior is perfectly followed at temperatures few degrees above T_{SO} and the fittings give the effective moment $\mu_{eff} = 8.30 \pm 0.05 \mu_B/\text{f.u.}$ and Weiss temperature $\theta_p = -17 \pm 1.75 \text{ K}$ along all the main axes. Since, in the paramagnetic region, the system consists of the two different non-interacting spins V^{3+} and Gd^{3+} , the effective moments can be estimated through the relationship $\mu_{eff} = \sqrt{\mu_{eff}^2(V^{3+}) + \mu_{eff}^2(Gd^{3+})}$ [12]. Assuming that the spins of the V^{3+} and Gd^{3+} are in the ground state with $\mu_{eff}(V^{3+}) = 2.83 \mu_B$ (spin only, $S = 1$) and $\mu_{eff}(Gd^{3+}) = 7.94 \mu_B$, an effective moment $\mu_{eff}(GdVO_3) = 8.43 \mu_B$ is obtained, which is very close to the observed experimental value. A noteworthy feature in the FCC, FCW data is also on the magnetization reversal observed along the a -axis at two temperatures denoted as T_o and T_s in Fig. 2. The values of T_o and T_s are dependent on the applied field and also on whether it is derived from FCC or FCW. At large enough field, e.g. $H = 0.5 \text{ kOe}$, there is no magnetization reversal nor any anomaly around T_s and T_o (data not shown).

In Fig. 4, we present the magnetic isotherms of the compounds measured along the main axes at different temperatures. In the “*high*” field regime, we observe a change in the features of the magnetization curves. Below T_M , there appear the field induced transition(s) along the a - and b -axes and the hysteresis along all the main axes which become disappeared at temperatures above T_M . The details of the magnetic isotherms around the origin are blown up and displayed in Fig. 5. It can be seen that there is also a characteristic change in the behavior of the magnetic

isotherms at temperatures below and above T_M . Below T_M , we observe no remanent magnetization and coercivity (Fig. 5a). The remanent magnetization and coercivity develop noticeably along the a -axis at temperature above T_M (Fig. 5b, c, d) which result in the magnetization reversal observed only along this direction (Fig. 2). The coercivity at 110 K (close to T_{SO}) is even higher than that obtained at 50 K and 12 K. The increase of the coercivity with increasing temperature observed in $GdVO_3$ is in contrast with conventional magnets in which thermal energy should lead to the reduction of the coercivity.

Since the a -axis is a “*peculiar*” direction, we have carried out in more details with further measurements. Earlier, we have reported that, in many of the RVO_3 compounds, the *ZFC* magnetization can be seriously affected by a presence of the inevitable trapped field (TF) in the superconducting magnet of SQUID [11,12]. We have examined the TF carefully. Before each measurement, we ran the degauss sequence to minimize the TF, its absolute value is estimated to be less than 2 Oe. We can “*generate*” the TF with opposite sign just by reversing the sign of the magnetic fields in the degauss sequence. In Fig. 6, we present the *ZFC* data of the compound bound with positive TF (PTF) and negative TF (NTF). From the Figure, it can be seen that the transition temperature T_M separates the *ZFC* curves into two distinctively different behaviors. Below T_M , the *ZFC* magnetization always follows the direction of the applied field in which it is being measured (hereafter denoted as H_{meas}). The two *ZFC*_PTF and *ZFC*_NTF curves (almost) coincide to each other (inset of Fig. 6). This observation is consistent with the fact that, below T_M , the compound does not have coercivity (Fig. 5a). When warming through T_M , the magnetization direction is no longer bound to the direction of H_{meas} , but to the TF under which the sample had been cooled previously. It means that, in this case, the magnetization direction can

memorize its previous state and behaves accordingly to it, i.e. the magnetic memory effect.

In order to explore this feature further, we carry out two different measurement protocols named as PA and PB. In PA, we first cool the sample in either PTF or NTF to 1.8 K. At this temperature, we start to “train” the sample by applying different magnetic field up to 50 kOe. The field is then switch to H_{meas} (chosen as 50 or 10 Oe), and the data are taken following the temperature sweep-up. In Fig. 7, we display the results corresponding with cooling in PTF (7a, 7c), and NTF (7b, 7d). In each Figure, the data of the no-training *ZFC* curve bound with an opposite TF are also added for comparison. In the insets of the Figure we have included also expanded views of the data at temperatures below T_M to indicate that, in this region, there is hardly any effect of the TF as well as the training fields on the obtained data. When warming the sample through T_M , the training field clearly shows its effect through different jumps in the sign and magnitude of the magnetization. With increasing the training field, we observed systematically that the jump is suppressed to make the two *ZFC*_PTF and *ZFC*_NTF curves to behave towards each other. The jump of the magnetization at T_M in a certain H_{meas} , thus, can be controlled through the training field.

In another measurement protocol PB, we first cool the sample in different magnetic fields (i.e. FC). Then at 1.8 K, the magnetic field is switched to H_{meas} (chosen as 100 Oe, 50 Oe or 10 Oe), and the data are taken following the temperature sweep-up. In Fig. 8, we display the results with cooling in positive field (8a, c, e) and negative field (8b, d, f). We note that at a certain H_{meas} , the FC_PTF and FC_NTF in Fig. 8 are exactly the same as the *ZFC*_PTF and *ZFC*_NTP with “no-training” in Fig. 7, respectively. We have also included, in the insets of Fig. 8, the extended views of the data below T_M , to indicate that, in this temperature region, the different cooling

fields hardly have any effect on the obtained results. When warming through T_M , it is again obvious that the different cooling fields systematically result in different jumps in the sign and magnitude of the magnetization. In this case, it is clear that the jump of the magnetization at T_M in respect to H_{meas} can be controlled both by the sign and the magnitude of the cooling field.

IV. DISCUSSIONS

The magnetic memory effect observed in GdVO_3 is very puzzling. Since it is only shown up through a magnetization jump at a single transition temperature T_M , the feature is distinctively different with other magnetic memory systems including spin glass [19] nanomagnetic particles [20] and phase separated manganites [21]. In the latter cases, aging and rejuvenation effects are usually being involved. Earlier, studies on GdVO_3 polycrystalline sample [15] reported a transition at 7.5 K (close to T_M of 8 K in our crystal) which was referred to as the antiferromagnetic Néel temperature of the compound. Recently, Miyasaka et al. [1] reported the heat capacity results for GdVO_3 single crystal which also shows three transitions as in our heat capacity data. The transition at T_M , however, was not discussed into details in their work.

From the magnetic isotherms at 1.8 K in Fig. 4a, we can see that the magnetization is “*saturated*” above applied field of about 40 kOe with a slight anisotropy in the magnetization values obtained along different axes. The saturation magnetization obtained at 50 kOe is of about $6.7 \mu_B/\text{f.u.}$ Since this value is very close to a theoretical value of $7 \mu_B$ for a Gd^{3+} free ion and much larger than $2 \mu_B$ for a V^{3+} free ion, it is reasonable to think that all of the Gd moments have been forced parallel at field of 50 kOe and they contribute mostly to the saturation magnetization obtained. The V^{3+} moments, on the other hand, are strongly antiferromagnetically coupled, as revealed by the high value of T_{SO} and the negative Weiss temperature. Thus the

applied field, which is at least two orders of magnitude smaller than the V-V AF superexchange interaction, should not have any significant influence on the vanadium moments. This scenario, however, can hardly account for the field induced magnetic phase transitions observed at low temperature for the compound, taking into account the fact that Gd^{3+} has S spin character with no crystalline anisotropy and its behavior under the magnetic field should be relatively simple. Obviously there should be some “extra” factors, e.g. related to V^{3+} magnetism, to account fully for the anomalous behavior of the magnetic isotherms at 1.8 K.

The importance of the V^{3+} magnetism is also being revealed through the magnetic memory effect at T_M . The transition at T_M , is clearly not just only due to the “trivial” AF ordering of the Gd moments. Apart from the magnetic memory effect, we also note that coercivity and remanent magnetization can develop only at temperatures above T_M . Previously, we have proposed that these latter features as well as the magnetization reversal should be originated from the inhomogeneous nature of the compound due to OQF [11,12]. According to our model, then the transition at T_M should also be related to the fact that the compound is changed from an inhomogeneous V^{3+} antiferromagnetism to a homogeneous one at lower temperature which apparently does not own any coercivity and remanent magnetization. To let it happen, we would speculate that there should be a (significant) JT lattice distortion caused by the AF ordering of the Gd moments at T_M and so it can suppress the effect of OQF of V^{3+} ions. In here, the question of how come the homogeneous AF phase can memorize its history at T_M remains elusive. In any case, the magnetic memory effect observed in $GdVO_3$ compound would suggest that the magnetic state below T_M is to be characterized by different configurations of the magnetic domains in which each configuration has a specific link to sample’s history. Such a different domain

configuration in homogenous AF phase depending on the history of the sample was observed previously for YMnO_3 [22] even though with no such of the magnetic memory effect as in the case of GdVO_3 .

V. CONCLUSIONS

In summary, we have studied the magnetic properties of the GdVO_3 single crystal. The compound has been shown to exhibit very rich magnetic properties including low field sensitive character, field induced phase transitions, magnetization reversal and magnetic memory effect. The latter is a unique feature of GdVO_3 among other orthovanadate compounds and it is distinctively different with many other magnetic memory systems such as spin glass, magnetic nano particles and the phase separated maganites. The controllable magnetization switch in both direction and magnitude may make the compound a potential material for constructing some spin valve devices. We have suggested that the compound is homogenously AF at low temperature but it can have different configurations of domains which show up differently through the magnetization jump at T_M . Further experiments, e.g. neutron diffraction to determine the magnetic structure, optical spectroscopy to visualise the domains, as well as theoretical consideration are needed to shed light on this interesting magnetic memory phenomenon.

ACKNOWLEDGEMENTS

We gratefully acknowledge support from EPSRC, UK.

References

1. S. Miyasaka, Y. Okimoto, M. Iwama and Y. Tokura, Phys. Rev. B, **68**, 100406 (2003).
2. C. Ulrich, G. Khaliullin, J. Sirker, M. Reehuis, M. Ohl, S. Miyasaka, Y. Tokura and B. Keimer, Phys. Rev. Lett., **91**, 257202 (2003).

3. G. Khaliullin, P. Horsch and A.M. Oleś, Phys. Rev. Lett., **86**, 3879 (2003).
4. Y. Motome, H. Seo, Z. Fang and N. Nagaosa, Phys. Rev. Lett., **90**, 146602 (2003).
5. Z. Fang and N. Nagaosa, Phys. Rev. Lett., **93**, 176404 (2004).
6. N. Shirakawa and M. Ishikawa, Jpn. J. Appl. Phys., **30**, L755 (1991).
7. A.V. Mahajan, D.C. Johnston, D.R. Torgeson and F. Borsa, Physica C, **185-189** 1095 (1991); Phys. Rev. B, **46**, 10966 (1992).
8. Y. Kimishima, Y. Chiyonagi, K. Shimizu and T. Mizuno, J. Magn. Magn. Mater., **210**, 244 (2000); Y. Kimishima, S. Nishida, T. Mizuno, Y. Chiyonagi and M. Uehara, Sol. State Comm., **122**, 519 (2002).
9. Y. Kimishima, M. Uehara and T. Saitoh, Sol. State Comm., **133**, 559 (2005).
10. Y. Ren, T.T.M. Palstra, D.I. Khomskii, E. Pellegrin, A.A. Nugroho, A.A. Menovsky and G.A. Sawatzky, Nature, **396**, 441 (1998); Y. Ren, T.T.M. Palstra, D.I. Khomskii, A.A. Nugroho, A.A. Menovsky and G.A. Sawatzky, Phys. Rev. B, **62**, 6577 (2000).
11. L.D. Tung, Phys. Rev. B, submitted (2005).
12. L.D. Tung, Phys. Rev. B, **72**, 054414 (2005).
13. Y. Kimishima, M. Takahashi, K. Okada, H. Ishikawa and Y. Chiyonagi, J. Magn. Magn. Mater., **140-144**, 1185 (1995).
14. T. Sakai, G. Adachi, J. Shiokawa and T. Shin-ike, J. App. Phys., **48**, 379 (1977).
15. R.M. Bozorth, H.J. Williams and D.E. Walsh, Phys. Rev., **103**, 572 (1956).
16. Through out the paper, we use *zero* and *ZFC* in italics to indicate that we ignore the small trapped field in the SQUID superconducting magnet.
17. McIlvried and McCarthy, Penn State University, University Park, Pennsylvania, ICDD Grand-in-Aid, (1974) (x-ray data base file ID 25-0205).

18. V.G. Zubkov, G.V. Bazuev and G.P. Shveikin, *Sov. Phys. Solid State*, **18**, 1165 (1976).
19. V. Dupuis, E. Vincent, J.-P. Bouchaud, J. Hammann, A. Ito and H.A. Katori, *Phys. Rev. B.*, **64**, 174204 (2001).
20. M. Sasaki, P.E. Jönsson, H. Takayama and H. Mamiya, *Phys. Rev. B*, **71**, 104405 (2005).
21. P. Levy, F. Parisi, L. Granja, E. Indelicato and G. Polla, *Phys. Rev. Lett.*, **89**, 137001 (2002).
22. M. Fiebig, D. Fröhlich, S. Leute and R.V. Pisarev, *J. App. Phys.*, **83**, 6560 (1998).

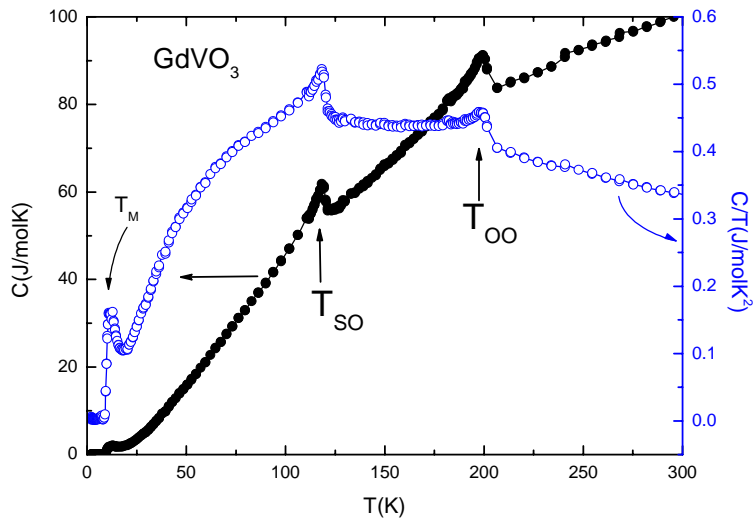


Fig. 1 (colors online): Heat capacity C and C/T as a function of temperature of the GdVO_3 single crystal.

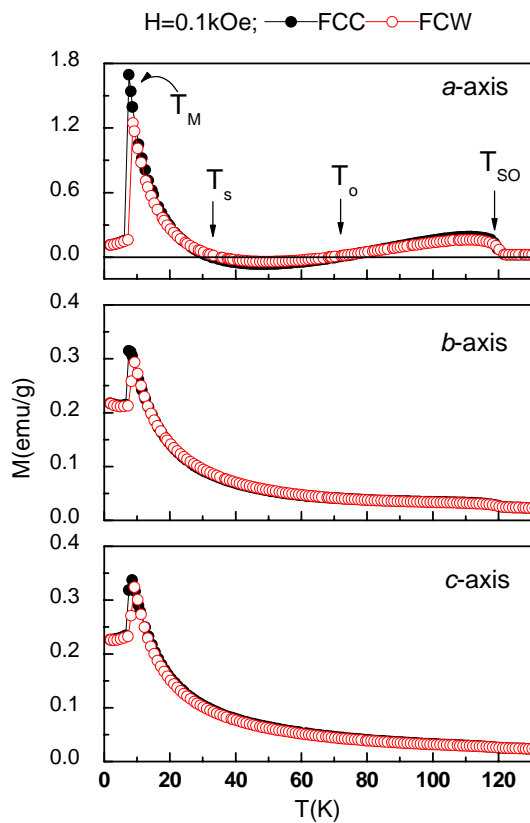


Fig. 2 (colors online): FCC, FCW magnetization of the GdVO_3 single crystal measured at 0.1 kOe along the main axes.

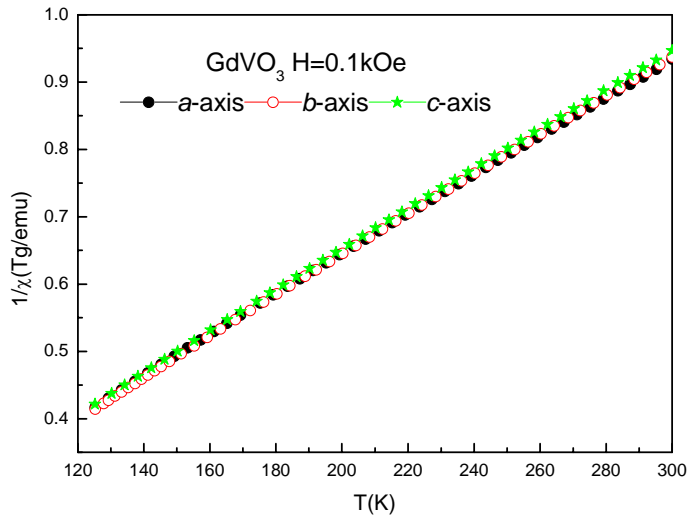


Fig. 3 (colors online): Temperature dependence of the inverse susceptibility in the paramagnetic region of the GdVO₃ single crystal.

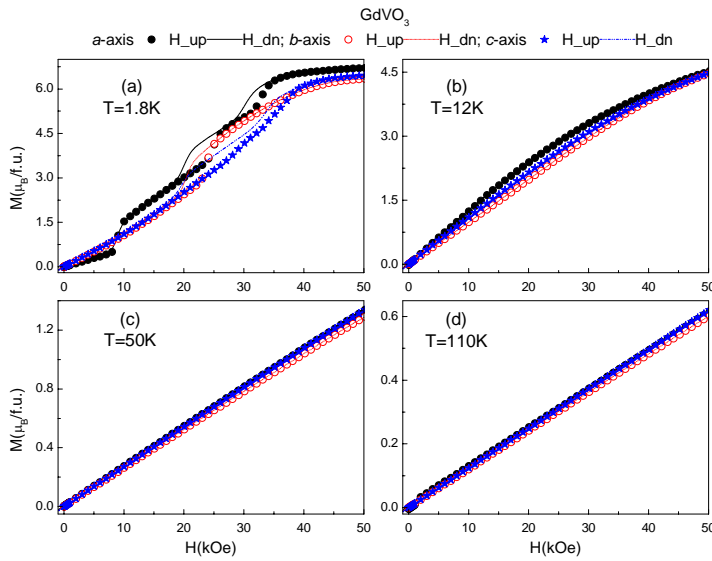


Fig. 4 (colors online): The magnetic isotherms of the GdVO₃ single crystal measured along the main axes at different temperatures: 1.8 K (a); 12 K (b); 50 K (c) and 110 K (d). The symbols correspond with increasing field sections, lines with decreasing sections.

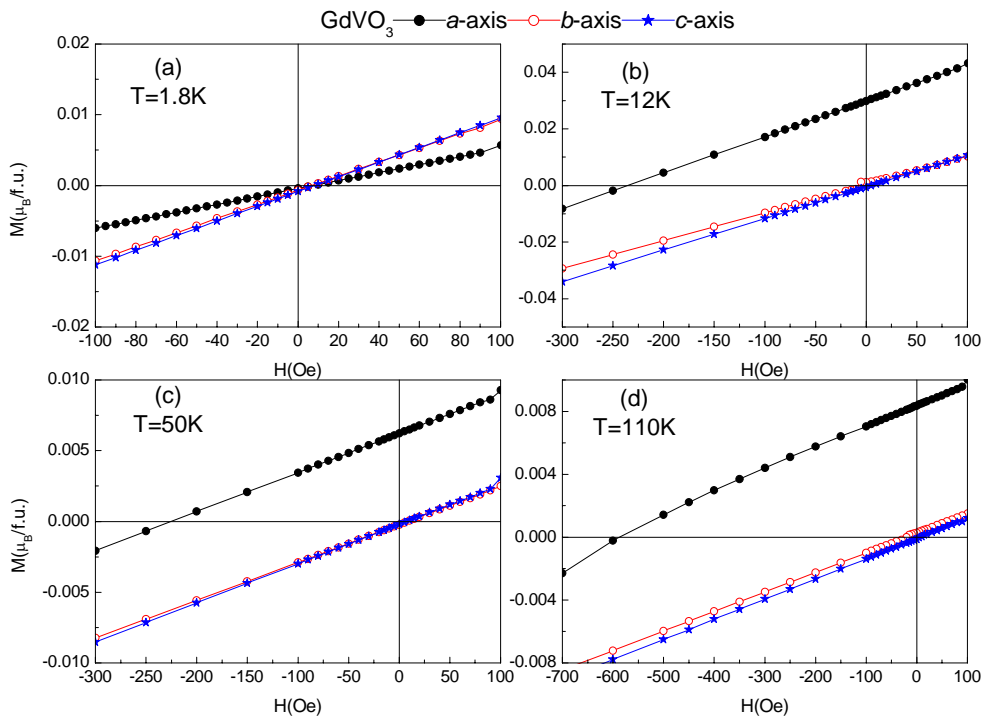


Fig. 5 (colors online): The expanded views around the origin of the decreasing field sections of the magnetic isotherms of the GdVO_3 single crystal measured along the main axes at different temperatures: 1.8 K (a); 12 K (b); 50 K (c) and 110 K (d).

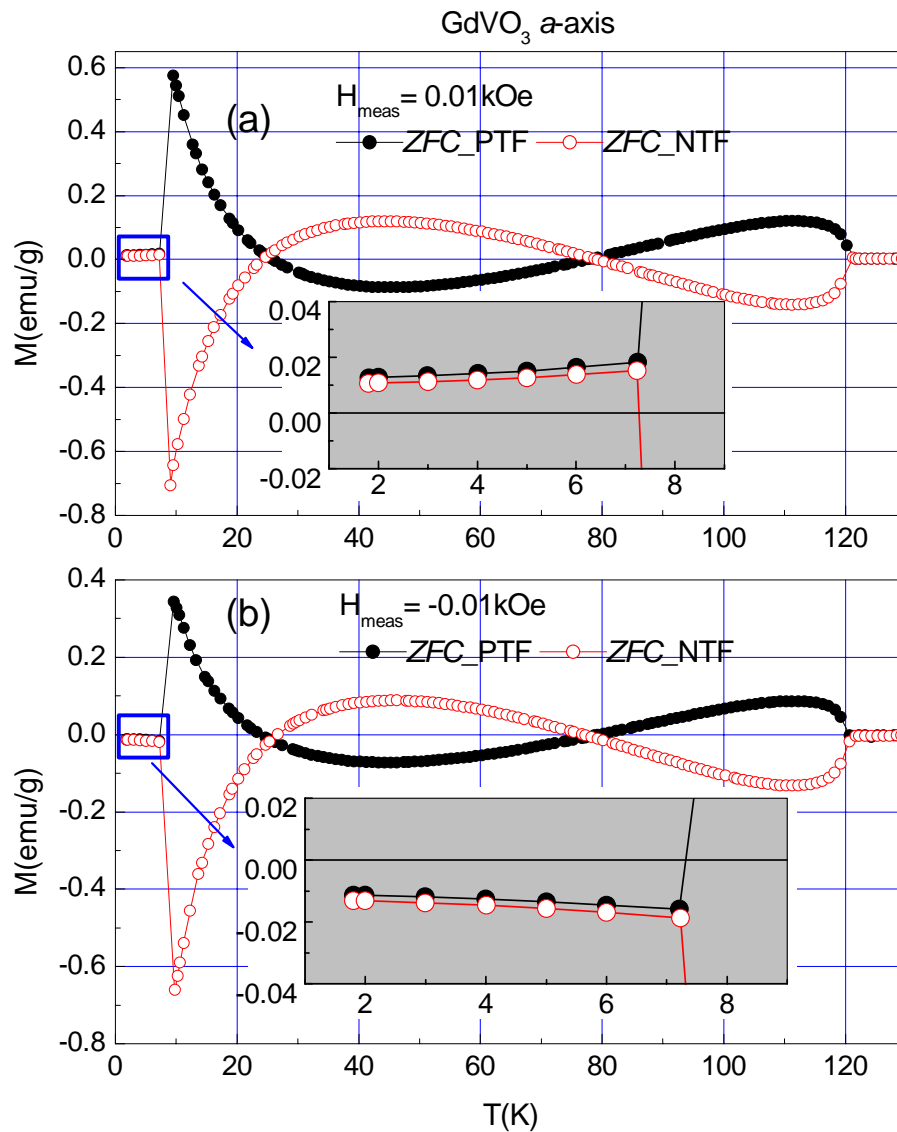


Fig. 6 (colors online): Effect of the trapped field on the *ZFC* magnetization measured along the *a*-axis of the GdVO_3 single crystal in applied field H_{meas} of 10 Oe (a) and -10 Oe (b). The inset shows an expanded view in the temperature region below T_M .

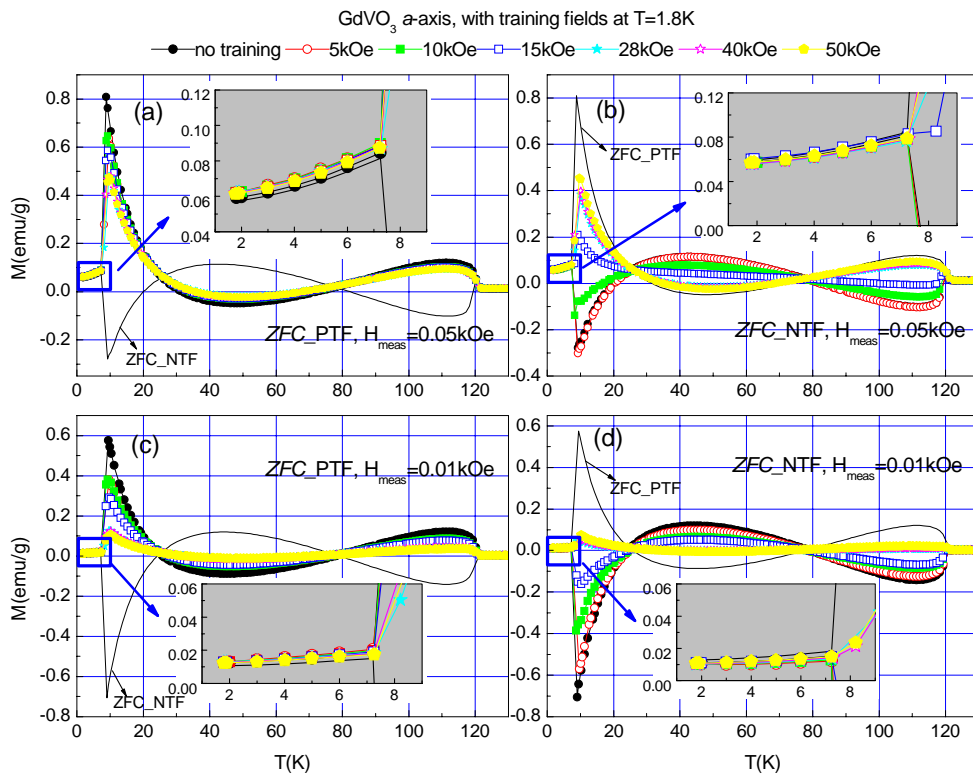


Fig. 7 (colors online): Effect of the training fields at 1.8 K on the temperature dependence of the ZFC_PTF (left panels) and ZFC_NTF (right panels) measured in different applied fields H_{meas} of 50 Oe (top), 10 Oe (bottom) along the *a*-axis of the GdVO₃ single crystal. The inset shows an expanded view in the temperature region below T_M .

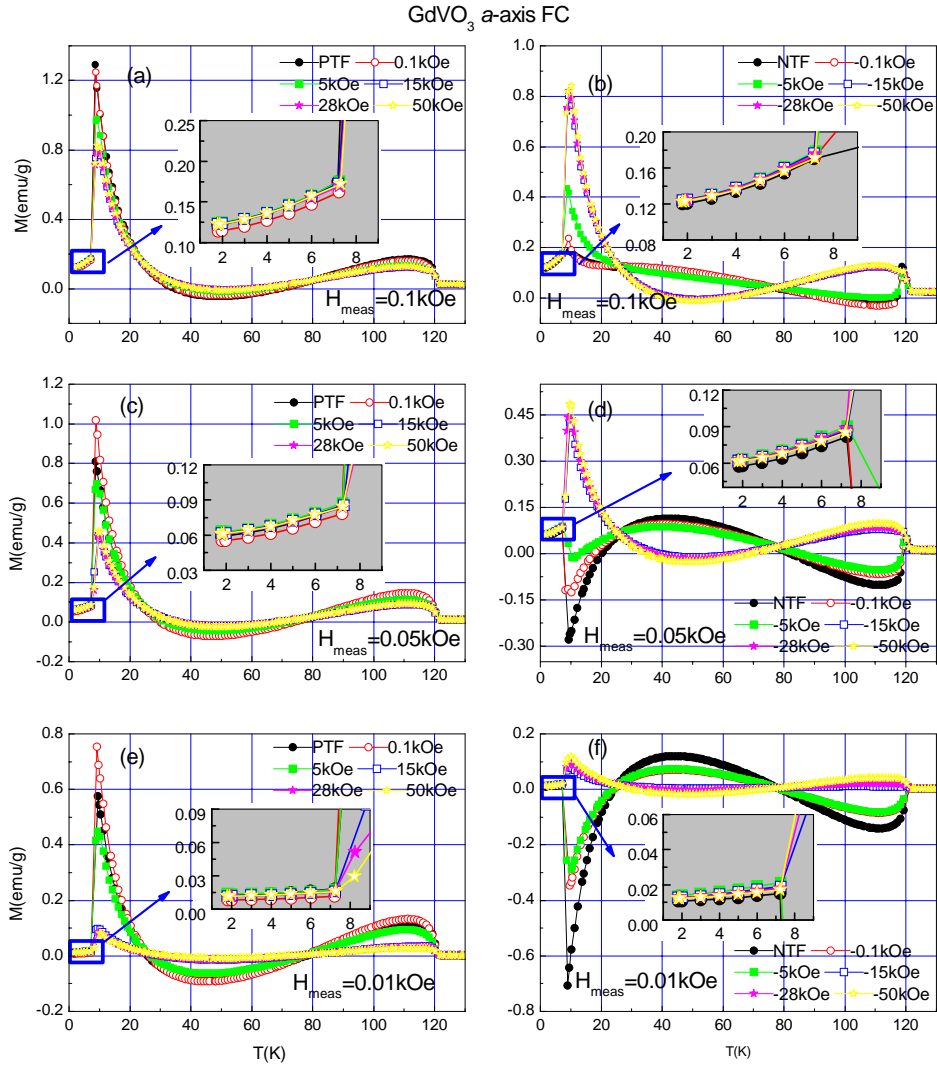


Fig. 8 (colors online): Effect of different cooling fields (positive fields on the left panel, negative fields on the right panel) on the temperature dependence of the magnetization measured in different applied fields H_{meas} of 100 Oe (top), 50 Oe (middle), 10 Oe (bottom) along the a -axis of the GdVO_3 single crystal. The inset shows an expanded view in the temperature region below T_M .